Chapter 13

Development of ($\lambda \sim 9.4\,\mu\mathrm{m}$) GaAs-Based Quantum Cascade Lasers Operating at the Room Temperature

Kamil Kosiel, Anna Szerling, Maciej Bugajski, Piotr Karbownik,
Justyna Kubacka-Traczyk, Iwona Sankowska, Emilia Pruszyńska-Karbownik,
Artur Trajnerowicz, Anna Wójcik-Jedlińska, Michał Wasiak, Dorota Pierścińska,
Kamil Pierściński, Shubhada Adhi, Tomasz Ochalski, Guillaume Huyet

Abstract The development of ($\lambda \sim 9.4\,\mu\mathrm{m}$) GaAs-based quantum cascade lasers (QCLs) operating at the room temperature is reported. The laser design followed an "anticrossed-diagonal" scheme of Page et al. [1]. The QCL GaAs/$Al_{0.45}Ga_{0.55}As$ heterostructures were grown by solid source (SS) MBE. The double trench lasers were fabricated using wet etching and Si_3N_4 for electrical insulation. Double plasmon confinement with Al-free waveguide has been used to minimize absorption losses. Optical and electrical properties of resulting devices are presented and discussed.

13.1 Introduction

The well-established GaAs/AlGaAs system has proved to be an attractive choice for quantum cascade lasers (QCLs), as it makes accessible the coherent emission in mid/far-infrared (IR) up to THz region. The growth of the heterostructures, however,

Kamil Kosiel, Anna Szerling, Maciej Bugajski, Piotr Karbownik, Justyna Kubacka-Traczyk,
Iwona Sankowska, Emilia Pruszyńska-Karbownik, Artur Trajnerowicz, Anna Wójcik-Jedlińska,
Dorota Pierścińska, Kamil Pierściński
Institute of Electron Technology, Al. Lotników 32/46, 02-668 Warszawa, Poland
(e-mail: kosiel@ite.waw.pl)

Michał Wasiak
Institute of Physics, Technical University of Łódź, Wólczańska 219, 93-005 Łódź, Poland

Shubhada Adhi
Department of Applied Physics and Instrumentation, Cork Institute of Technology, Ireland
Tyndall National Institute, Lee Maltings, Cork, Ireland
Department of Instrumentation Science, University of Pune, India

Tomasz Ochalski, Guillaume Huyet
Department of Applied Physics and Instrumentation, Cork Institute of Technology, Ireland,
Tyndall National Institute, Lee Maltings, Cork, Ireland

places extreme requirements on the individual layer thickness and composition as well as the overall periodicity of the whole structure.

The laser structures studied in this paper were the 36-period sequence of injector + 3QW active region, made of $Al_{0.45}Ga_{0.55}As/GaAs$ coupled quantum wells [2–4]. The application of relatively high Al content in AlGaAs layers, and hence the significant height of barriers, improves the thermal performance of the devices [2], in comparison with the earlier AlGaAs/GaAs QCL construction [5]. The injector doping, applied for only two barrier–QW pairs in the central part of each injector, has been tested in the range $n_i \sim 0.4$–2.2×10^{12} cm^{-2} per period. The structures doped to at least $n_i \sim 1 \times 10^{12}$ cm^{-2} have yielded lasing devices. The structure used double-plasmon Al-free waveguide for planar optical confinement.

The essential features of the considered design are anticrossed-diagonal transitions from pumped state to the lower laser state and depopulation of lower state by resonant optical phonon emission and tunneling into the injector. The lifetime of the excited state as well as dipole matrix element estimated close to laser threshold are reported in [2].

13.2 Experimental

The laser structures were grown by MBE in Riber Compact 21T reactor. The elemental beams were generated by using the ultrapure sources (6N5 Al, 7N Ga and 7N5 As). The beams of group III elements were produced from the standard ABN 80 DF effusion cells. The beam of As_4 molecules was generated by the valved cracker As effusion cell. The (100) oriented GaAs n+ substrates, rotated during epitaxy, were used. The temperature of the growing crystal surface T_s, controlled by a pyrometer, was kept at 580°C. The value of V/III ratio was at least 35 for the heterostructure growth. The heterostructures were grown without interruptions between adjacent layers. Detailed analysis of the growth optimization procedures can be found in [3, 4].

The laser operation is possible only when the designed structure is strictly realized, with the extreme technological precision concerning geometrical and doping features. To calibrate growth rates of consisting binaries, an appropriate complex procedure has been developed. It has in particular employed the RHEED oscillations technique as well as X-ray diffractometry (XRD) of test superlattice structures. For the analysis of $2\theta/\omega$ profiles (i.e., for simulating the symmetric (004) reflections) the dynamical diffraction theory has been used. Figure 13.1 presents the series of experimental diffraction curves for a number of consecutive growth runs compared to theoretical curve for attempted structure. Run-to-run module thickness reproducibility of about 1% was achieved. The reciprocal space map analyses confirmed the lack of extended defects in the grown structures.

The double-trench lasers were fabricated using wet etching and Si_3N_4 for electrical insulation [6]. The low resistivity Ni/AuGe/Ni/Au ohmic contacts, alloyed in
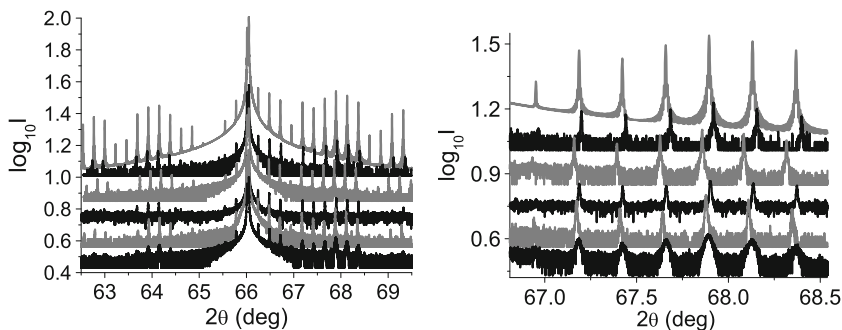
Fig. 13.1 Comparison of the experimental and simulated HRXRD $2\theta/\omega$ scans for grown QCL structures. The topmost curve is a simulated one. All wafers, except the bottom one, yielded lasing devices. Numerous satellite peaks confirm the high regularity of the active region structure. Their sharpness, representative for working structures, confirms the smooth interfacial morphology

430°C, were used at the top of the devices. For current injection, windows were opened through the insulator with width 15, 25 and 35 μm. After the wafer was thinned down to $\sim$100 μm, an alloyed AuGe/Ni/Au contact was deposited on the backside. The lasers were of 0.5, 1, 1.5 and 2 μm length and soldered epilayer down with Au/Sn eutectic, on diamond heatspreaders and copper heat sinks (Fig. 13.2). Alternatively the bars were soldered on heat sinks with indium. The influence of the indium thickness on the temperature of laser's active region was investigated by microphotoluminescence mapping (Fig. 13.3). It was proved that thinning the solder layer improves the thermal properties of laser.
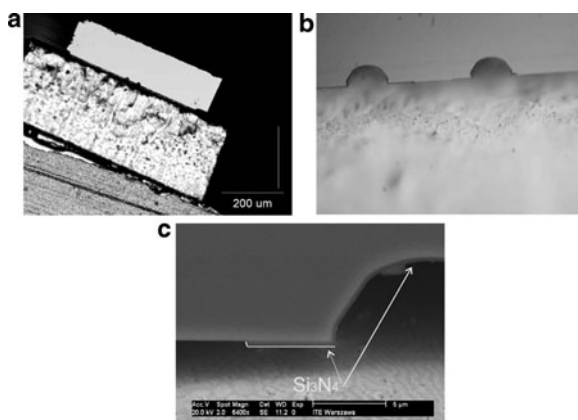

Fig. 13.2 SEM image of the device. (a) View of the device on diamond heatspreader. (b) Close-up view of the ridge of the device. (c) Note that Si_3N_4 insulating layer extends over a few micrometers on the top of the ridge to confine gain region

The basic electrical and optical characterization was carried out in the operating temperature range from 77 to 300 K. The laser emission was recorded with TE cooled HgCdTe detector (type PVI-2TE-10-Vigo System S.A.). Light from the laser was shined directly on the detector (no collimating lens was used).

13.3 Properties of the Lasers

The current-voltage characteristics, obtained for the structures in which the thickness and composition of active region layers were correctly engineered, are characterized by specific features (see Fig. 13.4(a)). At low bias QCL structures should be highly resistive. When the electric field reaches the value for which the alignment of the pumped laser state and the injector ground state takes place, electrons start
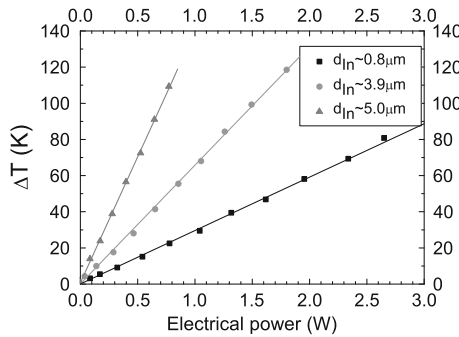

Fig. 13.3 The increase of the temperature of lasers' active region as a function of applied electrical power, for different thicknesses of indium used for soldering the lasers
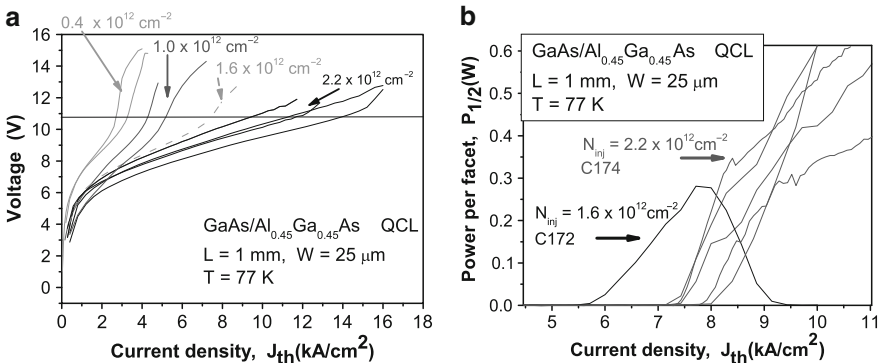

Fig. 13.4 (a) 77 K voltage-current (V–I) characteristics for a set of $Al_{0.45}Ga_{0.55}As/GaAs$ QCLs with different injector doping level (0.4–2.2×10^{12} cm^{-2} per period). Lasers were driven by 2 μs pulses with repetition rate of 0.5 kHz. (b) Light–current (P–I) characteristics for lasers with different injector doping; mirrors were uncoated

flowing through the device. In this regime the operating voltage increases linearly with injection current. The saturation of the V–I characteristics, i.e., the high differential resistance of the device, is caused by the onset of misalignment between the upper laser level and the injector ground state. The above description should match the results of V–I measurements performed at low operating temperature (77 K); for higher temperatures the lower values of device differential resistance at all current regimes are observed are as a rule.

The properties of the structures strongly depend on injector doping concentration n_i [4, 6]. The effect of saturation limits the dynamic range of laser operation. As the threshold condition may be reached only after the gain exceeds the losses, it is possible that the saturation condition may appear before the losses are exceeded. That is why to achieve lasing the high enough currents must flow through the structure before the saturation, and this requirement has to be fulfilled by a proper injector doping. As the initially applied injector doping ($\sim 0.4 \times 10^{12}\,\text{cm}^{-2}$) was found to be too low to achieve lasing, the range of higher injector doping was tested for a fixed QCL geometrical construction. It occurred that much higher currents before the saturation were necessary for lasing, and hence the injector doping had to be increased substantially (at least to $\sim 1.0 \times 10^{12}\,\text{cm}^{-2}$) – see Fig. 13.4(b).

In low operating temperature range the rise of n_i leads to increase of saturation current (I_{sat}) as well as threshold current (I_{th}), however I_{sat} rises faster (Fig. 13.4(a)). Hence the width of dynamical working range of current, and the resulting peak output power increases with n_i (Fig. 13.5(a)). The maximum operating temperature (T_{max}) also increases with n_i (Fig. 13.5(b)), because for higher n_i the rise of I_{th} with temperature is slower (Fig. 13.6(a)).
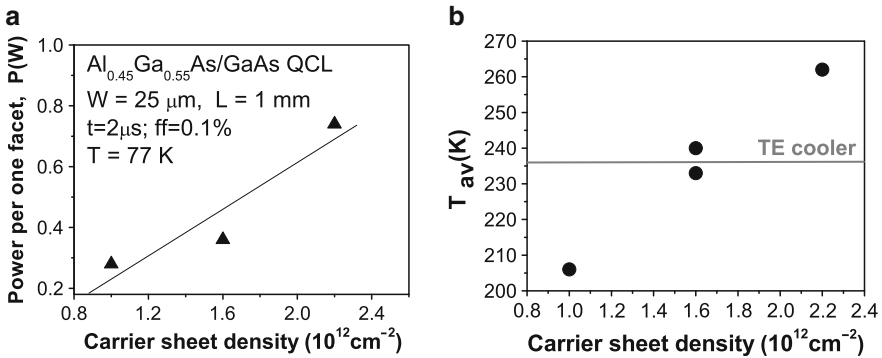

Fig. 13.5 Dependence of average output power for uncoated mirror (averaged for over 60 devices) on: (a) n_i, and (b) average T_{max} dependence on n_i

For $n_i \sim 2.2 \times 10^{12}\,\text{cm}^{-2}$ the average values of output power and efficiency (η) were 0.74 W and 0.85 W/A, respectively (the laser's mirrors were uncoated and thus power and η refer to one mirror; data are for $T = 77$ K and duty cycle ff $= 0.1\%$. The record output power was > 1 W (Fig. 13.6(b)). The corresponding average threshold current density was $J_{\text{th}} = 7.74\,\text{kA/cm}^2$. The stimulated emission has been observed
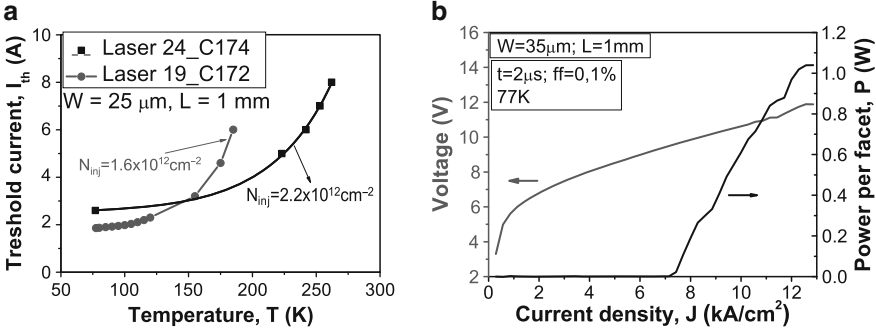
Fig. 13.6 (a) Operating temperature dependence of I_{th} for lasers with different n_i. Lasers were driven by 25 ns pulses with repetition frequency of 440 Hz. (b) Light–current and current-voltage characteristics of the laser. Output powers refer to uncoated facet
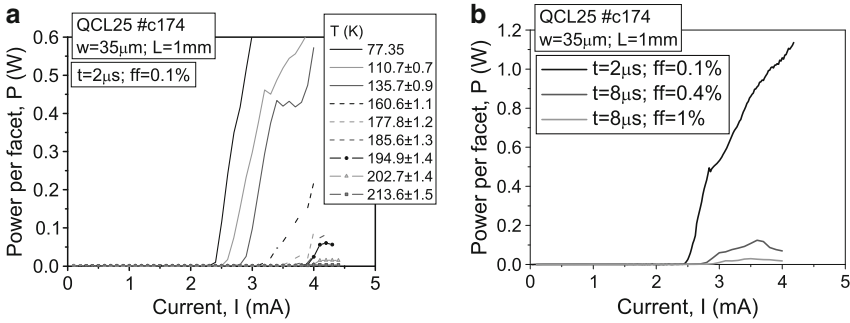

Fig. 13.7 (a) 77 K light–current (P–I) characteristics of the GaAs/Al$_{0.45}$Ga$_{0.55}$As laser at different operating temperatures. (b) Light–current characteristics for different pulse width at the repetition rate of 0.5 kHz

up to 1% duty cycle, 8 μs pulse duration (Fig. 13.7(b)). The lowest average $J_{th} = 4.8 \, \text{kA/cm}^2$ has been achieved for the lowest injector doping ($n_i \sim 1 \times 10^{12} \, \text{cm}^{-2}$). The above mentioned data refer to the lasers with window widths $\geq 25 \, \mu\text{m}$, resonator lengths $\leq 1 \, \text{mm}$, and with uncoated mirrors. The QCL threshold current density can be calculated from the equation [7]:

$$J_{th} = \frac{\varepsilon_0 n \lambda L (2\gamma_{32})}{4\pi e \Gamma |z_{32}|^2} \frac{\alpha_w + \alpha_m}{\tau_3 (1 - \tau_{21}/\tau_{32})} \tag{13.1}$$

where an injection efficiency of unity in the upper laser level E_3 is assumed and direct tunneling processes out of levels E_2 and E_3 are neglected. In this equation, ε_0 is the vacuum permittivity, n is effective refractive index of the laser mode, λ is the emission wavelength, L is the length of one segment, $2\gamma_{32}$ is the full width at the half maximum (FWHM) of the spontaneous emission spectrum and is directly related to the quality of the interfaces, e is the electron charge, Γ is the confinement factor for

whole active region, z_{32} is the dipole matrix element of the laser transition, and α_w are the waveguide losses. The scattering times τ_{ij} from states i to j are dominated by LO-phonon emission [7]. The mirror losses $\alpha_m = -\ln(R_1 R_2)/(2L)$ depend on cavity length and mirror reflectivities. For uncoated mirrors $R_1 = R_2 \approx 0.29$. The confinement factor Γ is estimated to be equal to 0.27 and the effective refractive index n is 3.27 [8]. For the investigated design $\lambda = 9.4\,\mu$m and $\tau_{32} = 2.1\,$ps.

The analysis of the above equation with numerical values of parameters as given in [1] shows that to provide modal gain at least $20\,\text{cm}^{-1}$ at the room temperature we need inversion $\sim 3 \times 10^{10}\,\text{cm}^{-2}$ (Fig. 13.8(a)), which should allow for threshold current densities in the range 3–$4\,\text{kA/cm}^2$ at $77\,$K in good quality devices ($\gamma_{32} = 12$–$14\,$meV) – see Fig. 13.8(b). The output power strongly depends on operating temperature as well as on supply conditions (Figs. 13.7 and 13.9). Light–current characteristics of the laser fabricated from GaAs/Al$_{0.45}$Ga$_{0.55}$As heterostructure with injector doping $\sim 2.2 \times 10^{12}\,\text{cm}^{-2}$, measured for long pulse operating conditions are shown in Fig. 13.7(a), where in particular the strong dependence of peak output power on duty cycle is seen. For very short pulses ($\lesssim 100\,$ns) however, the devices can tolerate relatively high pulse frequencies (up to $10\,$kHz), (Fig. 13.9(b)). This fact corresponds also with the pulse width influence on I_{th} and on the characteristic temperature T_0 value (Fig. 13.10(a)). The dependence of output power on supply conditions is followed by the corresponding dependence of T_{max} (Fig. 13.10(b)). The characteristic temperatures T_0 for the investigated lasers were typically of the order of $200\,$K and higher, which is value comparable with reported in literature (Fig. 13.10(a)).
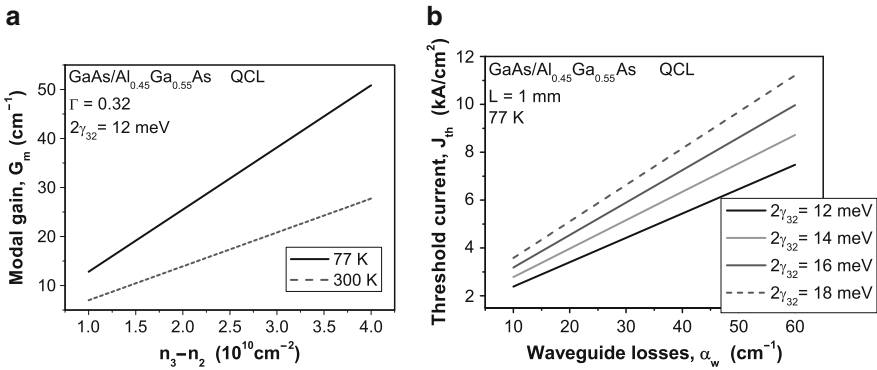

Fig. 13.8 (a) Modal gain vs. inversion, (b) threshold current density vs. waveguide losses for different values of γ_{32} parameter

To avoid excessive heating the decreasing of ridge width below $20\,\mu$m turned out to be necessary. Though, however, it allowed to increase the maximum operating temperature by a few tens of degrees in comparison with wider chips, the high reflectivity (HR) metallic (Al$_2$O$_3$/Au/Al$_2$O$_3$) coatings for back mirrors were necessary for obtaining the room-temperature operation (Fig. 13.11). The lasers emitted
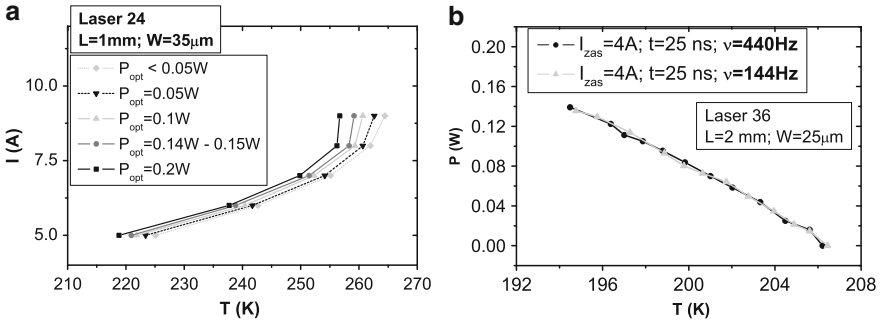
Fig. 13.9 (a) Dependence of supply current needed to maintain a certain output power on operating temperature. Laser was driven by 25 ns pulses with repetition frequency of 440 Hz. (b) Dependence of output power on operating temperature, for different supply conditions (lasers fed with very short pulses). Note the lack of output power dependence on pulse repetition rate for the fixed pulse width. The output power dependence on the pulse width with no dependence on repetition rate was observed in the short pulse regime (up to about 100 ns)
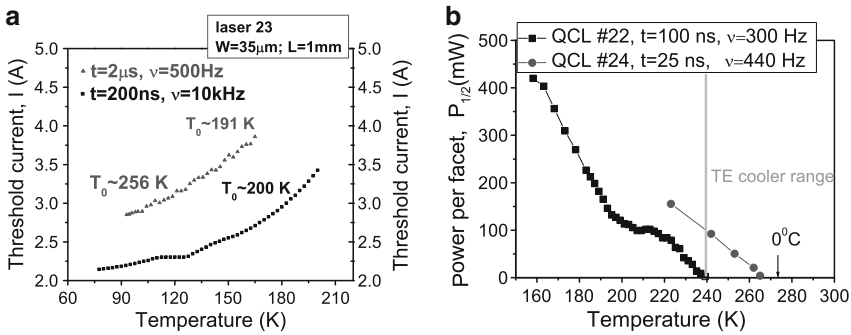

Fig. 13.10 (a) Temperature dependence of I_{th} for different supply conditions; note the two temperature ranges with different T_0 values. For shorter pulses the lower I_{th} was registered, in spite of higher duty cycle; this example emphasizes the significance of pulse duration. For long pulses (of the order of μs) I_{th} was always observed to rise with increasing duty cycle. (b) Output power for uncoated facet versus operating temperature; note the output power of the order of tens of mW in the range facilitated by two-stage TE Peltier coolers. Data collected for two different supply conditions – the higher T_{max} is for laser driven with shorter pulse width

at ∼9.4 μm in a single transverse mode. The spectrum consisted of a number of equally spaced longitudinal modes with mode spacing 1.47 cm^{-1} at 77 K and the full width at the half maximum of ∼0.26 cm^{-1} – see Fig. 13.12(a). With the increase of temperature the spectrum shifts towards the lower wavenumbers, with the rate of ∼0.1 cm^{-1}/K – see Fig. 13.12(b).
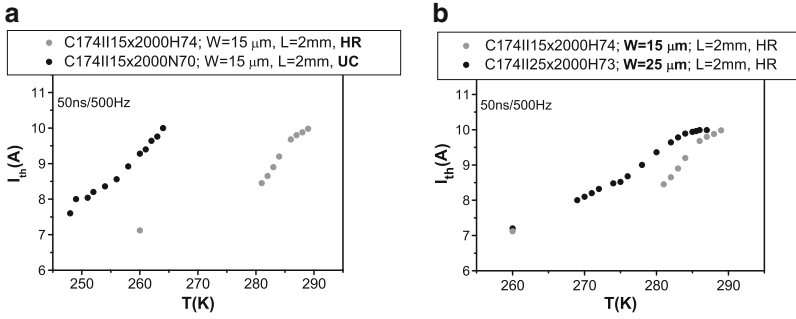
Fig. 13.11 (a) The temperature dependence of the threshold current for lasers with uncoated mirrors and with HR coating. (b) The same as above but for different resonator widths. Data in figure (b) is for lasers with HR coatings
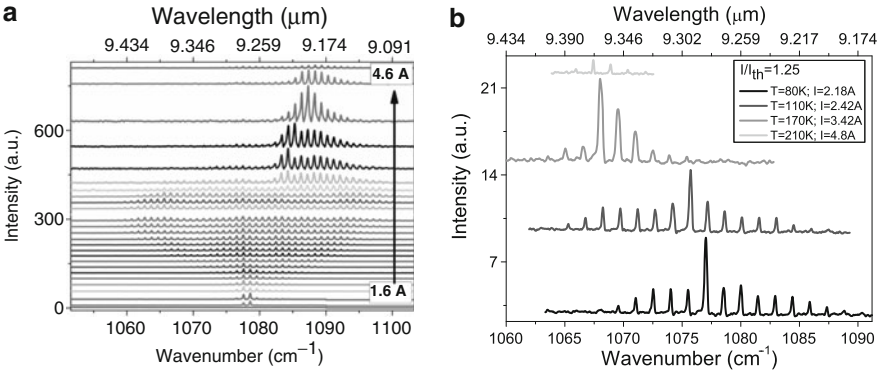

Fig. 13.12 Emission spectra for QCLs driven by pulses 50 ns and repetition 5 kHz; (a) for different values of supply current at 77 K, and (b) for different operating temperatures

13.4 Summary

In conclusion, the GaAs-based QCLs were developed emitting $\sim 1\,\text{W}$ peak optical powers at 77 K, and lasing with power of $\sim 12\,\text{mW}$ at the room temperature. An almost perfect matching of thicknesses ($\sim 1\%$) and compositions of individual layers was the prerequisite of QCLs lasing. However the RT operation was possible only on condition of ensuring high enough doping of injectors (at least to $\sim 1.0 \times 10^{12}\,\text{cm}^{-2}$), appropriately narrow ($\sim 15\,\mu\text{m}$) ridges and covering the back mirrors with high reflectivity coatings.

References

[1] H. Page, C. Becker, A. Robertson, G. Glastre, V. Ortiz, C. Sirtori, Applied Physics Letters **78**, 3529 (2001)

[2] K. Kosiel, M. Bugajski, A. Szerling, J. Kubacka-Traczyk, P. Karbownik, E. Pruszyńska-Karbownik, J. Muszalski, A. Łaszcz, P. Romanowski, M. Wasiak, W. Nakwaski, I. Makarowa, P. Perlin, Photonics Letters of Poland **1**, 16 (2009)

[3] K. Kosiel, J. Kubacka-Traczyk, P. Karbownik, A. Szerling, J. Muszalski, M. Bugajski, P. Romanowski, J. Gaca, M. Wójcik, Microelectronics Journal **40**, 565 (2008)

[4] K. Kosiel, A. Szerling, J. Kubacka-Traczyk, P. Karbownik, E. Pruszyńska-Karbownik, M. Bugajski, Acta Physica Polonica A **116**, 806 (2009)

[5] C. Sirtori, P. Kruck, S. Barbieri, P. Collot, J. Nagle, M. Beck, J. Faist, U. Oesterle, Applied Physics Letters **73**, 3486 (1998)

[6] A. Szerling, P. Karbownik, K. Kosiel, J. Kubacka-Traczyk, E. Pruszyńska-Karbownik, M. Płuska, M. Bugajski, Acta Physica Polonica A **116**, S45 (2009)

[7] H. Liu, F. Capasso (eds.), *Intersubband transitions in quantum wells: physics and device applications II* (Academic Press, 2000), chap. Quantum cascade lasers, p. 38. Semiconductors and Semimetals

[8] S. Höfling, R. Kallweit, J. Seufert, J. Koeth, J. Reithmaier, A. Forchel, J. Crystal Growth **278**, 775 (2005)